Prabha Materials Science Letters
Vol. 5, No. 2, 338-361, 2026
https://doi.org/10.33889/PMSL.2026.5.2.019

Microstructural Characterization of CNSL Based Natural Fibre Composites Using SEM and EDS Techniques

Samant Gaurish Mahabaleshwar
Mechanical Engineering Department,
Goa College of Engineering, Goa University, Farmagudi, 403401, Ponda, Goa, India.
Corresponding author: gms1.p22@gec.ac.in

Rajesh S. Prabhu Gaonkar
Mechanical Engineering Department,
Goa College of Engineering, Goa University, Farmagudi, 403401, Ponda, Goa, India.
E-mail: rpg@gec.ac.in

(Received on November 27, 2025; Revised on April 29, 2026 & June 3, 2026; Accepted on June 17, 2026)

Abstract
This study uses scanning electron microscopy (SEM) and energy dispersive spectroscopy (EDS) to develop an in depth understanding of the structural property of cashew nutshell liquid (CNSL) based composites reinforced with local natural fibres like Stocksii bamboo, areca nut leaf and coconut mid rib. Quantifiable SEM data were combined with elemental profiling across key microstructural regions to assess the effectiveness of chemical treatments, fibre matrix interfacial bonding, failure mechanisms, nano filler, and microstructural changes during manufacturing. Alkaline treatment reduced fibre diameter and increased surface roughness, consistent with the selective removal of hemicellulose and waxy layers as confirmed by EDS. Silane treatment produced polymerised interphase, reflected in an 18.6% reduction in silicon and a 79% rise in sulphur content, establishing complementary chemical and mechanical bonding mechanisms. It was observed that Interfacial quality has significantly improved, with contact length increasing from 67.3% in untreated natural fibres to 93.1% in the treated fibres, supported by maximum interfacial oxygen and sulphur accumulation. A significant change from brittle pullout failure in untreated composites to fracture dominated behaviour in treated systems was observed by fractography analysis, which clearly correlated with improved interfacial bonding. Incorporating nano filler which resulted in a distinctive triple phase fibre matrix nanofiller interface with higher oxygen of 44.27 wt%, silicon with 9.42 wt%, and calcium concentration of 6.5X, which resulted into improved fracture toughness. Manufacturing method comparison exhibited that compression moulding produced the most refined microstructure comparative to vacuum bagging and hand layup. It was observed that significant linear association between tensile strength and interfacial contact length, showing that mechanical parameters can be effectively estimated from microstructural observations. Overall, the SEM EDS analysis shows that CNSL based natural fibre composites could achieve interfacial bonding and microstructural integrity similar to synthetic polymers. These results show that CNSL based green composites are both economically and technologically viable as high performing, sustainable materials obtained from renewable resources.

Keywords- Cashew nutshell liquid, Alkali and silane treatment, Natural fibre, SEM and EDS analysis.

1. Introduction

SEM analysis collective with corresponding EDS signifies the most influential unified analytical approach for inclusive composite microstructural characterization, allowing direct visualization and quantitative elemental profiling of fibre matrix interfaces at nanometer to micrometer scales (Sanjay et al., 2018; Zhou et al., 2014). Compared to conventional optical microscopy, which is limited to micrometer resolution, SEM generates high resolution surface images that displayed minute details of interfacial boundaries, surface topography, phase distributions, and critical processing-induced defects (Madhusudhana et al., 2021). By simultaneously identifying all elements present and measuring their concentration at specific microstructural locations, EDS X-ray analysis offers chemical level insight into interfacial composition and nano filler architecture (Lee et al., 2021). Natural fibre reinforced polymer

composites represent emerging sustainable alternatives to glass fibre composites, offering environmental advantages through renewable resource utilization, biodegradability, and reduced carbon footprint (Goda et al., 2024). However, fundamental incompatibility between hydrophilic natural fibre surfaces and hydrophobic polymer matrices necessitates chemical surface treatments to optimize interfacial adhesion (Thomason, 2022). Cashew nutshell liquid (CNSL), a bio based thermoset resin derived from agricultural waste, presents promising matrix material for ecofriendly composites but requires detailed microstructural investigation to validate interface quality and performance potential (Parveen et al., 2013).

Chemical treatments including alkaline and silane chemical treatment substantially modify the fibre surface's morphology by eliminating surface contaminants and adding reactive functional groups (Guo et al., 2023). The addition of nano filler further changes the composite microstructure through superior interface accumulation and matrix property enhancement (Dhariwal & Banerjee, 2025). During manufacturing process there are some induced defects, fibre alignment, and void formation which notably affect the property of the composite material (Azad et al., 2024).

This detailed investigation establishes autonomous understanding of the subsequent topics through integrated SEM EDS analysis: (1) Chemical treatment effectiveness through morphological and elemental analysis; (2) Fibre matrix interfacial bonding enhancement through contact length quantification and elemental profiling; (3) Failure mechanism transitions through fractographic analysis correlated with interfacial bonding; (4) Nano filler preferential distinction and triple phase interface architecture; (5) Manufacturing technique effects on microstructural ; and (6) Quantitative structure property correlations enabling mechanical performance prediction (Kurpińska et al., 2022).

Relative with conventional optical imaging techniques, the combination of EDS and SEM imaging techniques offers a more comprehensive understanding of fibre matrix interactions. EDS enhances SEM by identifying the localized elemental composition across specific microstructural areas, while SEM provides high resolution imaging of surface morphology, interfacial gaps, fibre roughness, and fracture properties. Direct linkage between chemical and physical characteristics at the contact is made possible by this integrated method. This link is especially significant in natural fibre composites since both surface morphology and chemical compatibility affect interfacial performance. Thus, SEM and EDS analysis enable a thorough assessment of the surface modification of fibres following chemical treatments, the impact of processing methods on defect development, and the function of nano fillers in modifying interfacial architecture. This unified methodology provides a more solid foundation for understanding and enhancing structural property correlations in green composites. Because of their low density, biodegradability, and affordability, CNSL based natural fibre composites have potential uses in lightweight, structural components, packaging materials, car interior panels, and protective structures. These composites mechanical performance, durability, and appropriateness for such applications are directly influenced by their microstructural integrity and interfacial bonding properties. For example, higher fibre matrix adhesion improves load transfer efficiency and qualifies these materials for semi structural applications; increased dispersion and decreased void content lead to increased environmental resistance and reliability.

2. Materials and Methodology

2.1 Material Composition and Characterization

Natural fibres used for the composite fabrication include bamboo (Bambusa Stocksii), coconut mid rib, and areca leaf sheath shown in **Figure 1**, extracted from agricultural waste sources in Goa, India (Santhosha et al., 2023).

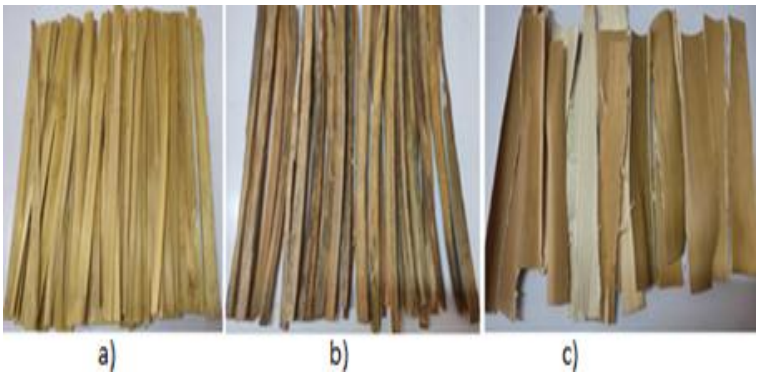

Figure 1. Raw natural fibres used in the composite fabrication: (a) bamboo fibre, (b) coconut leaf mid rib fibre, and (c) areca leaf sheath fibre.

Technical grade CNSL matrix consisted of anacardic acid of 70%, cardol of 20%, and cardanol approximately of 10%, with kinematic viscosity of 125 cSt at 40°C (Mahabaleshwar & Gaonkar, 2025). Chemical treatments: (1) Alkaline: 5% NaOH aqueous solution, 2 hours at 60°C; (2) Silane: 2% 3-aminopropyltriethoxysilane in 95% ethanol, 30 minutes at room temperature (Mehta et al., 2004; Niutta et al., 2023). Nano fillers incorporated at 1.5 to 2.5 wt % included single walled carbon nanotubes of 1 to 2 nm diameter, graphene of 2 to 5 nm thickness, and silicon dioxide nanoparticles with 5 to 10 nm diameter (Agresti et al., 2025). The samples manufactured using vacuum bagging technique, compression molding and hand layup technique.

2.2 SEM Specimen Preparation and Analysis

Composite samples shown in **Figure 2** were sectioned perpendicular to fibre alignment using precision diamond saw at 300 rpm (Gonçalves et al., 2025; Khot et al., 2001). Specimens were mounted on aluminum stubs using conductive double sided carbon tape and sputter coated with 10 to 15 nm gold palladium layer (60:40 ratio) at 20 mA for 120 seconds (Yadav et al., 2024). Carl Ziess Scanning Electron Microscope operating in secondary electron detection mode at 15 to 25 kV accelerating voltage (Junior et al., 2024). Magnification sequence is low magnification (100 to 500X) for composite overview; intermediate magnification (1000 to 5000X) for fibre topography and interface characterization; high magnification (10000 to 30000X) for detailed surface morphology and interfacial contact quantification (Alao et al., 2021). Quantitative measurements are fibre diameters; surface roughness parameters; void fraction percentage; fibre matrix interfacial contact length with minimum 20 interfaces/sample (Lionetto et al., 2012).

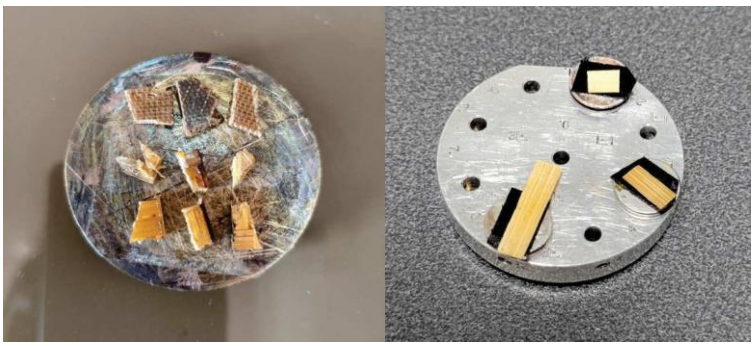

Figure 2. SEM specimens.

2.3 EDS Analysis Methodology

All EDS analyses employed EDAX TEAM software integrated with Carl Zeiss EVO 18 microscope. Standardized parameters are 20 kV accelerating voltage, 150 Nano amperes beam current, 38.2 to 39.7 seconds live time per analysis, 50° takeoff angle, 0.24 eV energy resolution (Sajin et al., 2022). Elemental quantification utilized eZAF Smart Quant correction algorithm providing automated atomic number (Z), absorption (A), and fluorescence (F) corrections (Salem et al., 2023). Results reported as both weight percentage and atomic percentage with quantification errors are major elements (Alam & Chowdhury, 2021).

2.4 Manufacturing Techniques

Composites were fabricated using three techniques: (1) Compression Molding: fibre and resin mixture in aluminum molds, 80 MPa pressure for 24 hours; (2) Vacuum Bagging: layered fibre and resin components in vacuum bag, 0.8 bar absolute pressure, room temperature cure 24 hours; (3) Hand Layup: manual fibre placement with resin application, atmospheric pressure ambient cure 24 hours shown in **Figure 3** (Pandian et al., 2014).

Figure 3. composite fabrication processes: (a) compression molding (b) vacuum bagging (c) hand layup process.

3. SEM and EDS Results

Comprehensive microstructural characterization through SEM combined with EDS analysis provides integrated understanding of fibre matrix interactions, nano filler architecture, and interfacial bonding governing CNSL based green composite performance (Sanjay et al., 2018; Zhou et al., 2014). This section presents detailed SEM morphological observations synchronized with quantitative EDS elemental composition data across distinct microstructural regions, establishing definitive structure-property correlations (Madhusudhana et al., 2021).

3.1 Fibre Surface Morphology and SEM Analysis

3.1.1 Untreated Natural Fibre Characteristics

SEM imaging of untreated bamboo fibres revealed smooth surface morphology interrupted by scattered impurities, wax, pectin, and hemicellulose residues appearing as amorphous white deposits (Wang et al., 2020). Average untreated bamboo fibre diameter is 18.5 ± 2.1 µm. Fibre surfaces displayed minimal surface roughness (Ra: 0.65 µm) with incomplete fibrillar structure exposure (Vydrina et al., 2023).

The SEM micrographs (**Figure 4** and **Figure 5**) provide a clear conception of the structural characteristics, surface defects, and underlying features of bamboo fibres prior to their integration into the CNSL matrix. At higher magnification, the bamboo fibre surface reveals well defined longitudinal fibrils, which run parallel to the fibre axis. These fibrillar structures highlight the natural multi layered arrangement of cellulose microfibrils within the bamboo vascular bundles, a feature responsible for its native tensile strength. However, despite the organized fibrillar architecture, several inherent surface irregularities are evident.

SEM images of untreated bamboo fibre show a relatively smooth (**Figure 4** and **Figure 5**) and compact fibrillar structure with minimal texturing. Longitudinal microfibrils are closely arranged, but areas of smooth waxy layers and pinned vascular holes are clearly visible. These natural features reduce resin wettability and create weak points in fibre matrix bonding. The presence of such impurities suggests that the untreated fibre surface offers limited mechanical interlocking and poor chemical affinity toward hydrophobic polymer matrices.

Untreated Coconut mid rib fibres (**Figure 6**) exhibit a distinctly porous, layered morphology composed of irregular cell walls and loosely bonded microfibrils. Numerous bulges, grooves, and surface cavities are observed, indicating inherent structural non uniformity. A noticeable waxy coating remains adhered to the surface, and the presence of micro cracks suggests susceptibility to moisture absorption and stress concentration.

Such characteristics highlight the need for surface treatment to stabilise and activate the fibre for composite application. The untreated Areca leaf sheath fibre (**Figure 7**) surface displays longitudinal microfibrils but includes prominent waxy deposits, smooth wall segments, and biological residues. The fibre surface appears relatively closed, with fewer open fibrils available for resin anchoring. Small pores and surface depressions are visible, reflecting the heterogeneous nature of lignocellulosic layers. These untreated features limit the development of strong interfacial adhesion.

Complementary EDS analysis of untreated coconut leaf petiole fibre revealed characteristic elemental composition dominated by oxygen (38.51 wt %, 53.39 at%) reflecting abundant cellulose, hemicellulose, and lignin constituents (Lauff et al., 2025). Secondary EDS elements included sodium (29.21 wt %, 28.18 at%) representing residual salt contamination, sulfur (9.60 wt %, 6.64 at%) indicating processing residues, and silicon (7.99 wt %, 6.31 at%) reflecting natural silica in fibre epidermis (Wolela, 2019). This integrated SEM EDS baseline establishes untreated fibre reference for morphological and chemical comparison with treated surfaces (Kushwaha & Kumar, 2010).

The overall performance of composite and interfacial bonding is governed by the surface properties of untreated natural fibres. From the SEM micrographs it has been noted that there are some surface contaminants like pectin, wax, and hemicellulose presence has been seen in fibres like coconut midrib, arecanut leaf sheath and bamboo. The contaminants create a challenge in order to get proper bonding between the matrix and reinforcement. These contaminants reduce the wettability of matrix material due to which the surface energy gets reduces. The flat surfaces of untreated fibres limit the mechanical interlocking and the inherent surface qualities of natural fibres like grooves, micro cracks and holes which results into stress concentration. Subsequently the reinforcement matrix interaction continues to weak, which results into ineffective stress transmission under the loading. Fractographic observations, which show dominating fibre pull-out and interfacial deboning in untreated composites, support this behaviour. To improve interfacial adhesion and boost composite performance, surface impurity removal and fibre shape modification are crucial processes.

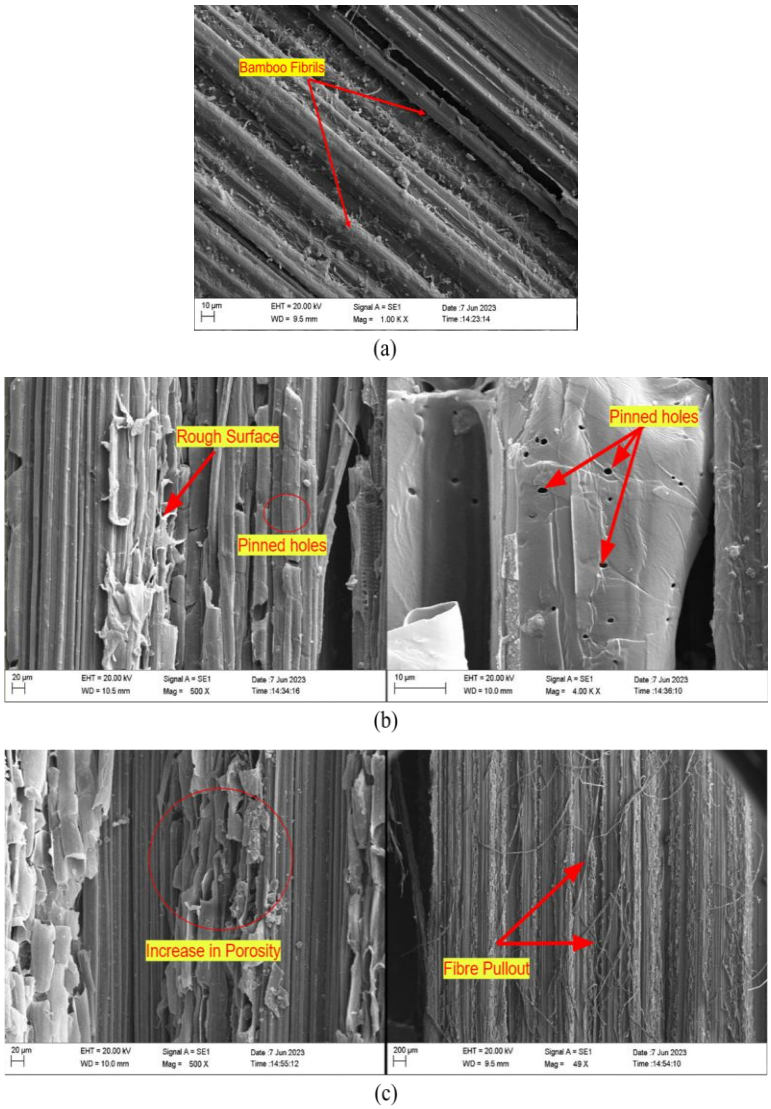

Figure 4. SEM images of bamboo fibres: (a) untreated fibre (b) alkali treated fibre (c) alkali silane treated fibre.

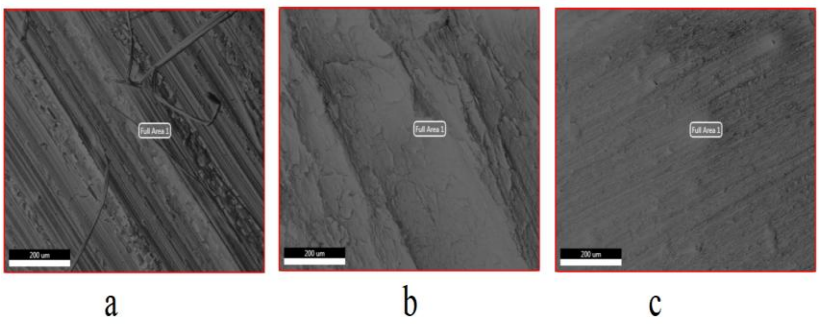

Figure 5. SEM images of bamboo fibre (a) untreated fibre (b) alkaline treated fibre (c) alkaline silane treated fibre.

Table 1. Comprehensive eds quantitative analysis for all areas (Weight %).

Element	Untreated fibre	CNSL matrix	Silane-treated	Fibre-matrix interface	Alk-Treated fibre	Alk-Silane fibre	Graphene matrix	CNT matrix	Triple-phase interface
O (wt %)	42.07	36.08	39.82	**52.10**	38.51	37.37	40.32	40.82	**44.27**
Si (wt %)	2.03	3.86	6.20	4.54	7.99	6.49	8.67	7.90	**9.42**
S (wt %)	50.56	0.00	14.50	15.30	9.60	**17.10**	14.15	12.15	16.10
Na (wt %)	—	1.22	2.10	8.03	29.21	16.78	17.45	19.06	12.64
K (wt %)	4.70	—	0.15	0.16	0.14	0.18	—	0.02	0.43
Ca (wt %)	0.40	1.23	2.40	2.81	2.18	2.59	5.21	6.38	**7.93**
Pb (wt %)	8.49	27.18	13.80	13.31	8.49	14.98	11.23	10.15	13.77
Mg (wt %)	0.03	—	1.85	2.16	3.35	3.36	—	3.30	3.23
Fe (wt %)	—	—	0.75	1.49	0.51	1.05	0.79	0.21	0.79
Cl (wt %)	—	—	0.06	0.10	0.03	0.09	—	0.01	0.09

3.1.2 Alkaline Treatment Induced Morphological and Chemical Transformation

After the natural fibres were obtained from mechanical processes it under goes alkali treatment with 5% NaOH concentration and deep into it for eight hours at 60°C, after that it was observed that bamboo fibre surfaces displayed prominently enhanced roughness with pronounced axial grooves and exposed fibrillar bundles, which confirms the hemicellulose and pectin removal from the natural fibres (Lu et al., 2000).

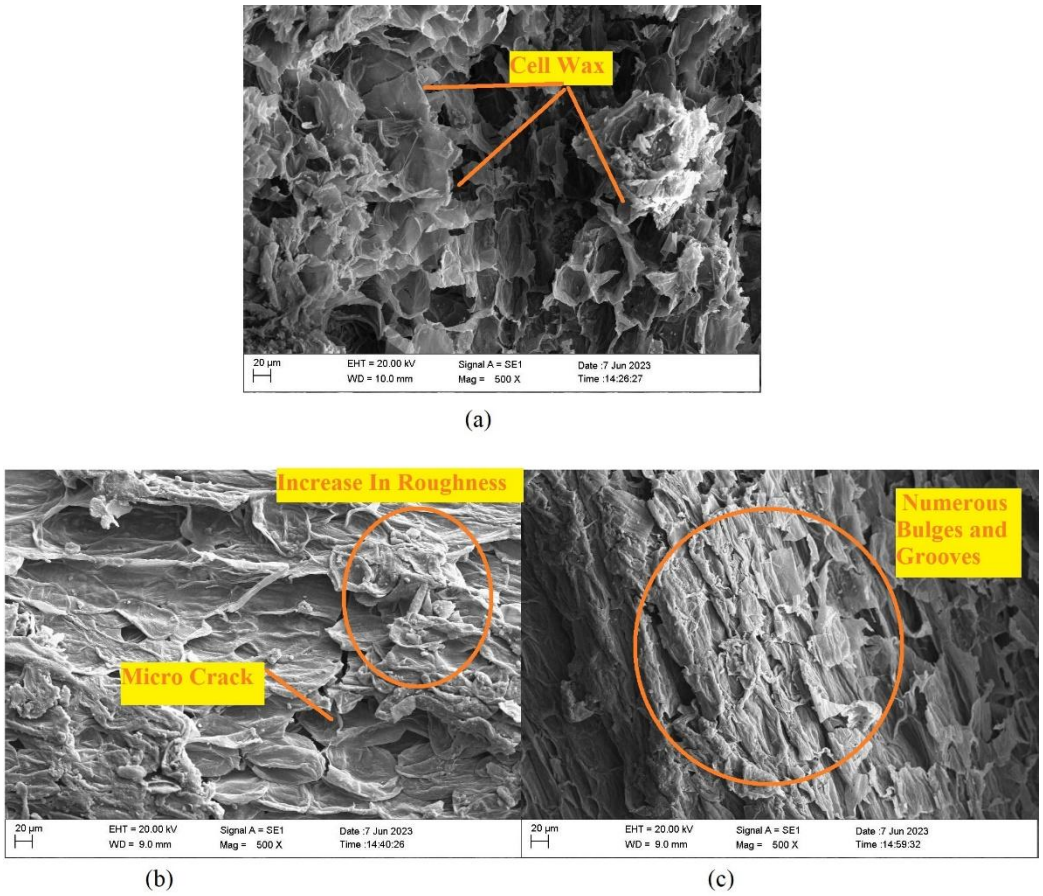

Figure 6. SEM images of coconut mid rib fibres: (a) untreated, (b) alkali-treated (c) Silane treated.

Quantitative SEM image analysis displays bamboo fibre diameter reduction of 22.3% (post treatment: 14.4 ± 1.8 μm); surface roughness parameter Ra increased from 0.65 μm (untreated) to 1.42 μm (alkaline treated), representing 118% roughness enhancement (Lu et al., 2000). Similar effects observed for areca fibres (13.2% diameter reduction, Ra: 0.58 to 1.28 μm; coconut petiole fibres it was observed that 18.7% diameter reduction, and surface roughness Ra from 0.71 to 1.35 μm (Bledzki & Gassan, 1999).

After the alkali treatment, the natural fibres like bamboo fibres show (**Figure 4**) clearer exposure of individual fibrils along with deeper grooves and micro roughness. The alkaline solution eliminates the hemicellulose, waxes, and surface impurities, making the fibre topography more open and rougher. The increase in roughness which enhances the potential of mechanical interlocking and substantially it improves interfacial compatibility with the resin matrix. Alkali treated Coconut mid rib fibres (**Figure 6**) exhibit a extreme change in surface morphology. The SEM images show the removal of waxy layers and exposure of open cell structures of the fibre. Numerous bulges and grooves appear more noticeable on the surface, suggesting the dissolution of non-cellulosic components. The fibre surface becomes rougher and more fibrillated, enhancing potential bonding between the fibre and matrix. Small micro cracks are visible after the treatment that is due to the partial removal of weaker amorphous regions from the fibre surface, which helps to activate the surface for improved adhesion with the resin material.

The alkaline treated Areca leaf sheath fibres (**Figure 7**) exhibit a substantial modification, with the disappearance of smooth waxy layers and emergence of open fibrillar bundles. Increased roughness, surface porosity, and longitudinal grooves demonstrate in effective removal of surface impurities from the surfaces of the fibre. These microstructural changes improve resin penetration into the fibres and promote stronger mechanical interlocking at the interface of matrix and reinforcement.

The EDS analysis of alkaline treated bamboo fibre reinforcement showed that oxygen is of 38.51 wt % and 53.39 at% remaining stable compared to untreated bamboo fibre, indicating selective removal of hemicellulose and pectin from the fibre while cellulose preservation occurred. Significantly, sodium remained elevated at 29.21 wt % and 28.18 at% confirming a complete 5% NaOH immersion effectiveness for eight hours at 60°C. Silicon content remained consistent of 7.99 wt % and 6.31 at% by demonstrating resilience of natural fibre silica layers to alkaline treatment (Fiore et al., 2020). The even elemental profile with residual sodium accumulation and unaltered silicon which confirms the alkaline treatment has successfully removed the surface impurities and hemicelluloses through saponification reactions without degrading core cellulose structure (Kaewkuk et al., 2010).

The very foremost information about the alkaline chemical treatment is selectivity is revealed by the EDS analysis results. The relatively constant silicon content shows that the natural silica in the natural fibre reinforcement structure is unchanged due to the treatment, which clearly shows that the treatment does not change the fibber's mineral constituents. Moreover, the steady oxygen concentration presence verifies that the cellulose backbone, which is abundant in functional groups that carry oxygen, is maintained during the chemical treatment. This proposes that NaOH chemical treatment mostly eliminates amorphous components like hemicellulose and pectin without weakening the natural fibber's structural integrity which is very much important to give strength to the composite. To achieve better mechanical properties and interfacial bonding without sacrificing mechanical performance, these results show that the alkaline treatment is selective and successfully modifies the fibre surface whereas sustaining its structural integrity.

The alkaline chemical treatment mechanism involves the following points (1) Pectin and wax dissolution through saponification process (2) Hemicellulose partial removal via alkali catalyzed ether bond cleavage

process (3) Lignin surface modification through de-polymerization process by exposing underlying cellulose structures with enhanced reactivity (Belgacem & Gandini, 2005; Butera et al., 2021).

The eradication of hemicellulose, pectin, and waxy surface layers from the natural fibres is directly related to the improvement in interfacial bonding between reinforcement and matrix following NaOH chemical treatment. These elements create an amorphous outer layer that restricts the contact between the reinforcement and matrix. When they are removed by the chemical treatment, the underlying cellulose microfibrils are seen, giving the surface a rougher, more textured appearance at the surface of fibre. SEM analysis observations display the formation of fibrillation at the surface, increased surface area due to roughness, and grooves that enable the resin to penetrate the matrix material, which results into the improvement of the fibre and matrix's mechanical interlocking. Additionally, the elimination of these non-cellulosic elements makes hydroxyl groups more accessible on the natural fibre's surface, which increases the wettability and fosters improved interfacial contact with the resin matrix materials. As a result, load transmission efficiency is increased and interfacial gaps are decreased, which improves the composite performance.

3.1.3 Silane Chemical Treatment Induced Surface Polymerization and Elemental Modification

When the alkaline chemical treated natural fibres are obtained which were treated with 2% APTES silane treatment for 30 minutes at room temperature. SEM images exhibited that the substantial additional surface modifications of natural fibre with characteristic nodular/granular texture representing a polymerized silane coupling agent formations. Silane chemical treatment overlayer thickness is from 50 to 150 nm confirmed by cross sectional edge analysis. Surface roughness has increased to Ra 2.15 μm for combined alkaline silane treated bamboo fibres, it was observed that 51% additional increase relative to the alkali treatment only, resulting from polymerized silane layer filling on the surface grooves while creating additional Nano scale roughness on the natural fibre (Subramanian et al., 1996).

SEM analysis of alkali silane treated bamboo (**Figure 4**) fibres reveals a more uniform and chemically activated surface. A thin polymerised silane layer fills micro voids and produces a smoother but functional surface. The deposition creates reactive sites for covalent bonding with the polymer matrix, reducing porosity and enhancing fibre matrix compatibility (Tomczak et al., 2007). Recent work in sustainable manufacturing also shows that ecofriendly processing media can significantly improve performance, further supporting the shift toward greener engineering solutions (Usgaonkar & Gaonkar, 2024; Usgaonkar & Gaonkar, 2025).

Silane treated Coconut mid rib (**Figure 6**) fibres show a stabilised and uniformly coated surface. The previously exposed rough zones appear more consolidated due to silane deposition, which bridges gaps between fibrils. Numerous SEM images remain visible, but the overall structure of the natural fibre appears more cohesive. This indicates improved chemical reactivity and favourable surface energy for bonding with CNSL resin.

The alkali silane treated Areca leaf sheath (**Figure 7**) fibres display a balanced morphology where the roughened fibrillar zones are uniformly coated with silane. After the treatment it was observed that localised bulges, grooves, pores, and porous regions appear are sealed or chemically stabilised. This uniform silane network which enhances the wetting of matrix and reduces the fibre hydrophilicity, also it improves the potential for both mechanical interlocking and covalent bonding between the reinforcement and matrix.

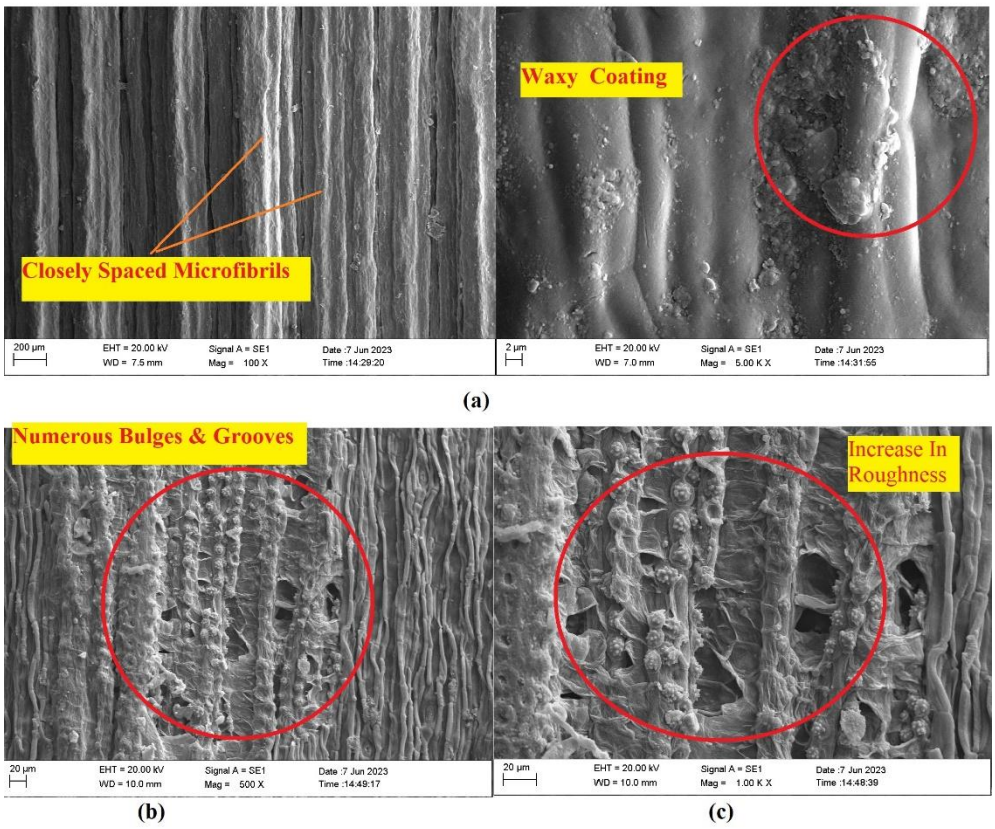

Figure 7. SEM images of Areca Leaf Sheath: (a) untreated, (b) alkali treated (c) alkali silane treated.

EDS analysis of combined alkaline and silane treated bamboo fibre exhibited a distinctive elemental signature confirming polymerized silane over layer formation on the bamboo fibres. Silicon content decreased from 7.99 wt % for untreated fibres to 6.49 wt % to alk-silane treated fibres, which represents 18.6% silicon reduction indicating to ~50 to 150 nm polymerized silane overlayer coating on the fibre surface. Sulfur intensely elevated from 9.60 wt % for untreated to 17.10 wt % to alkaline and silane treated, representing 79% increase, which confirms the sulfur containing silane coupling agent and sulfur modified matrix constituents preferentially accumulate on silane treated fibre surfaces, which enhances the interfacial bonding chemistry. Oxygen slightly decreased from 38.51 wt % for untreated fibres to 37.37 wt % for alkaline and silane treated fibres, reflecting polymerized silane over layer partial obscuring oxygen bearing fibre surface.

The silane treatment induces three mechanisms are as follows (1) The covalent bonding to fibre substrate through Si-O-C and Si-O-Si linkages with cellulose hydroxyl groups (2) Reactive functional group introduction available for resin matrix interaction (3) Surface energy modification reducing hydrophilicity and improving resin matrix wettability. Silane treated fibre surfaces display enhanced capability for matrix resin penetration into fibrillar structures, facilitating both mechanical interlocking and chemical bonding at the interface of reinforcement and matrix materials.

Table 2. Comprehensive EDS quantitative analysis for all areas (Atomic %).

Element	Untreated fibre	CNSL matrix	Silane-treated	Fibre-matrix interface	Alk-Treated Fibre	Alk-silane fibre	Graphene matrix	CNT matrix	Triple-phase interface
O (at%)	59.42	63.54	58.72	**72.34**	53.39	56.54	58.47	58.13	**61.12**
Si (at%)	1.63	3.88	5.12	3.59	6.31	5.59	7.29	6.41	**7.81**
S (at%)	35.64	0.00	11.84	10.60	6.64	**12.91**	10.15	8.63	11.37
Na (at%)	—	2.37	14.92	7.76	28.18	17.66	17.22	18.89	12.45
K (at%)	2.71	—	0.09	0.09	0.08	0.11	—	0.01	0.25
Ca (at%)	0.23	0.87	1.41	1.56	1.20	1.57	3.11	3.63	**4.68**
Pb (at%)	0.91	3.70	1.58	1.43	0.91	1.75	1.27	1.12	1.50
Mg (at%)	0.03	—	2.95	1.97	3.05	3.34	—	3.09	3.01
Fe (at%)	—	—	0.38	0.59	0.20	0.45	0.32	0.09	0.32
Cl (at%)	—	—	0.04	0.06	0.02	0.06	—	0.00	0.06

Table 1 and **Table 2** present the comprehensive quantitative elemental composition across all nine microstructural regions as determined by EDS analysis. The data reveals systematic elemental patterns directly correlating with microstructural analysis features and interfacial chemistry. Untreated fibre exhibits a high sulfur content of 50.56 wt %, characteristic of lignocellulosic material contaminants. Alkaline treatment reduces sulfur by 81% of 9.60 wt %, confirming effective removal of non-cellulosic impurities, while maintaining stable oxygen concentration of 38.51 wt % indicating selective hemicellulose removal with cellulose preservation. Combined alkaline and silane treatment produces characteristic signatures: sulfur elevation to 17.10 wt % which is +79% increase, silicon reduction to 6.49 wt % which is -18.6%, quantifying to ~50 to 150 nm silane over layer, and sodium accumulation of 16.78 wt %, residual chemical treatment.

The fibre matrix interface region exhibits a maximum oxygen concentration of 52.10 wt %, which confirms the concentrated fibre phase at the bonding zone, with elevated sulfur of 15.30 wt % indicating accumulation of sulfur containing bonding compounds. Nano filler enriched zones show distinctive elemental signatures which are graphene matrix with elevated silicon to 8.67 wt %, CNT matrix with maximum sodium of 19.06 wt % indicating surfactant incorporation, and Calcium concentration peaked at 7.93 wt % (4.68 at%), highest among all analyzed regions, representing 6.5X elevation compared to pure matrix of 1.23 wt %. These elemental patterns provide quantitative validation of treatment effectiveness, interfacial bonding optimization, and nano filler preferential accumulation mechanisms for the reinforcement and matrix interaction. The effects of silane and alkaline chemical treatments on fibre surface morphology and interfacial behaviour are clearly distinguished by SEM analysis. Alkaline chemical treatment increases the surface roughness, also exposes the fibrillar structures, and creates micro grooves by removing surface contaminants from the fibres such hemicellulose, pectin, and waxy layers. These modifications strengthen fibre matrix interaction and mechanical interlocking. By creating a thin polymerized interphase layer, silane treatment on the fibres, on the other hand, further alters the fibre surfaces. When surface irregularities are partially filled in while still retaining enough roughness on the surface, SEM images show a more homogeneous and stable surface. This layer enhances the compatibility and lowers interfacial flaws by encouraging chemical interaction between the fibres and matrix. In general, silane chemical treatment promotes chemical coupling, leading to a more effective and stable fibre matrix interface, while alkaline chemical treatment mainly improves physical adhesion through surface roughening.

3.2 Fibre Matrix Interfacial Bonding Analysis: SEM and EDS Correlation

3.2.1 Poor Adhesion Characteristics in Untreated Fibre Composites

Cross sectional SEM image analysis of composites material containing untreated bamboo natural fibres revealed poor interfacial contact characterized by (1) Numerous 0.5 to 5 μm interfacial gaps between reinforcement and the matrix; (2) Observable fibre de-bonding from matrix in fabricated specimens (3) Incomplete resin penetration into the fibre surface depressions. Quantitative SEM interfacial analysis for untreated bamboo fibre matrix contact length averaged 67.3% of theoretical maximum contact perimeter, indicating only ~67% of potential interfacial areas achieves direct molecular contact. Interfacial void fraction as ~2.8% in untreated fibre composites.

EDS analysis of pure CNSL matrix region identified characteristic thermoset resin elemental composition dominated by oxygen of 36.08 wt % and 63.54 at% which reflects cardanol and bio-based constituents. EDS analysis of the CNSL matrix region revealed that oxygen is the dominant element. In addition, the lead of 27.18 wt % and 3.70 at% was detected in the analyzed region. The presence of lead may be associated with additives, impurities, catalyst residues, pigments, or processing related to contaminants present in the resin system. However, the precise source of lead could not be conclusively determined from the present investigation and requires further study. The poor interfacial bonding in untreated fibre composites which results from the fundamental incompatibility between hydrophilic fibre surfaces containing abundant OH groups and hydrophobic CNSL matrix rich in aliphatic hydrocarbons with limited hydrogen bonding capability.

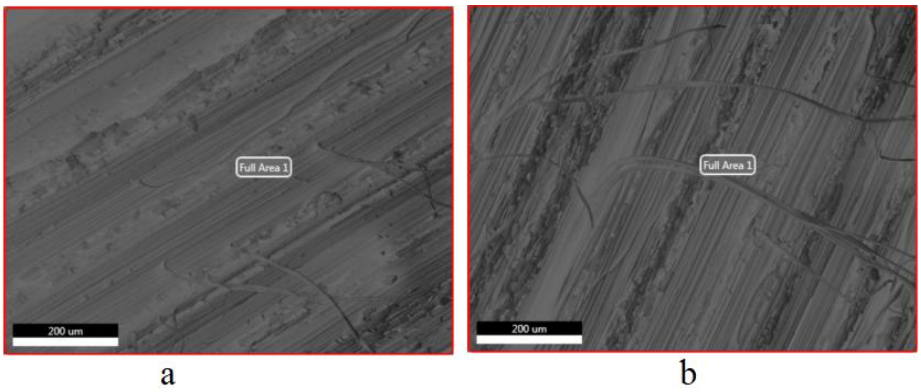

Figure 8. SEM images of fibre matrix interfaces (a) poor adhesion with interfacial voids in untreated composite, (b) optimized interfacial contact with minimal voids in alkaline silane chemical treated composite.

3.2.2 Enhanced Interface with Alkaline Treatment

The composite cross sections containing alkaline treated bamboo natural fibres displayed substantially enhanced interfacial characteristics are as follows (1) Reduced interfacial voids (2) Enhanced fibre wetting through increased mechanical interlocking with roughened fibre surfaces (3) Increased interfacial contact length to 81.7% of theoretical maximum. SEM elemental correlation for quantitative measurement of alkaline chemical treated fibre matrix interfaces reveals continuous matrix fibre contact across 81.7% of theoretical contact perimeter.

The mechanism underlying this improvement involves the following (1) Reduced fibre hydrophilicity via removal of OH groups from hemicellulose and surface impurities, which reduces the fibre moisture affinity from 12.3% of untreated to 8.1% of alkaline-treated; (2) Enhanced surface reactivity through

exposed cellulose hydroxyl group accessibility for interfacial interactions with CNSL groups (3) Mechanical interlocking optimization via increased surface roughness of 118% enhancement facilitating matrix material anchoring within fibre surface depressions. Comparable improvements documented for areca fibres of interfacial void reduction to 1.3%, and contact length increased to 80.2% and coconut mid rib fibres of void reduction to 1.2%, and contact length increased to 79.8%.

3.2.3 Optimized Interface with Combined Alkaline Silane Chemical Treatment and Interfacial Elemental Architecture

Composites incorporating combined alkaline and silane chemical treated fibres exhibited most favorable interfacial characteristics are as follows (1) Minimal interfacial voids of 0.5 to 0.7% void fraction (2) Intimate fibre matrix contact of contact length increases to 93.1% for bamboo fibres, approaching theoretical maximum (3) Formation of 50 to 100 nm interfacial transition zone with graduated composition.

EDS analysis of fibre matrix interface region revealed that characteristic interfacial elemental composition is distinct from both untreated natural fibre and matrix regions. Oxygen content reached to maximum value of 52.10 wt % and 72.34 at% across all nine analyzed regions, confirming interface represents concentrated fibre and carbohydrate phase transitioning to matrix dominated regions. Sulfur concentration elevated that 15.30 wt % of 10.60 at%, significantly higher than the untreated fibre of 9.60 wt % indicating that sulfur containing compounds preferentially segregate and accumulate at fibre matrix boundary during composite processing, enhancing interfacial bonding. Lead moderately concentrated to 13.31 wt % and 1.43 at%, showing intermediate composition between high lead matrix of 27.18 wt % and low lead fibre of 8.49 wt %, indicating gradual compositional transition zone.

Quantitative interfacial adhesion assessment for bamboo fibres achieves 93.1% theoretical contact, areca fibres for 91.8%, and coconut petiole fibres for 90.3%, representing average improvements of 38 to 43% relative to untreated fibre composites. This SEM EDS analysis correlation demonstrates progressive interfacial optimization through chemical treatment, with elemental profiling quantitatively confirming enhanced fibre matrix interface quality.

The silane coupling agent mechanism for interface improvement involves following (1) Chemical bridging of Si-O-C bonds to fibre substrate while NH_2 and CNSL groups orient toward matrix (2) Reduced interfacial tension from modified fibre surface energy and improving matrix wetting and flow into surface irregularities (3) Enhanced stress transfer via covalent bonding enabling effective matrix to fibre load transmission without interfacial slippage.

3.3 Fractographic Analysis and Failure Mechanism Characterization

3.3.1 Brittle Pull Out Dominated Failure in Untreated Fibre Composites

Tensile failure surfaces of untreated fibre composites exhibited characteristic brittle fracture morphology (1) Fibre pull out with minimal residual matrix material adhering to fibre surface (indicating weak fibre matrix bonding); (2) Brittle matrix cracking showing sharp fracture surfaces without plastic deformation evidence; (3) Void initiated fracture patterns with fracture emanating from interfacial voids. Quantitative SEM fractographic analysis for approximately 68-72% of fibre cross sections in tensile failure specimens exhibited clean pull out with <5% residual matrix coverage, confirming ineffective interfacial load transfer. Pull out fibre length analysis revealed short pull-out distances (5-50 μm), indicating minimal stress transmission to fibre phase.

As seen in **Figure 9(a)**, at a magnification of 3000X, a clear separation is visible between the fibre surface and the surrounding matrix material. This region of delamination suggests insufficient wetting or poor interfacial bonding between the fibre and the matrix material, leading to de-bonding under mechanical loading. The gap formation along the fibre boundary indicates that the fibre matrix adhesion was locally compromised, allowing the crack to propagate along the interface. **Figure 9(b)** shows the surface morphology of the matrix at 5000X magnification, where several micro cracks are visible across the resin layer. These cracks are indicative of brittle failure within the matrix materials, likely caused due to stress concentration or inadequate load transfer between the matrix and reinforcing natural fibres. The presence of these micro cracks confirms that the matrix region contributed significantly to the initiation and propagation of failure in the composite materials.

3.3.2 Transitional Failure Characteristics with Alkaline Treatment

Tensile failure surfaces of alkaline treated fibre composites displayed transitional failure characteristics are as follows (1) Reduced fibre pull out of 35 to 42% clean pull out; remaining of 58 to 65% exhibited which more than the 20% residual matrix coverage (2) Increased fibre fracture instances in tensile loading direction, indicating successful stress transfer to the fibres; (3) Evidence of localized matrix plastic deformation adjacent to fractured fibres. Pull out fibre lengths increased to 100 to 200 μm, demonstrating enhanced frictional load transfer. Matrix deformation patterns revealed microscopic shear yielding zones adjacent to fibre fractures, indicating matrix stress dissipation mechanisms.

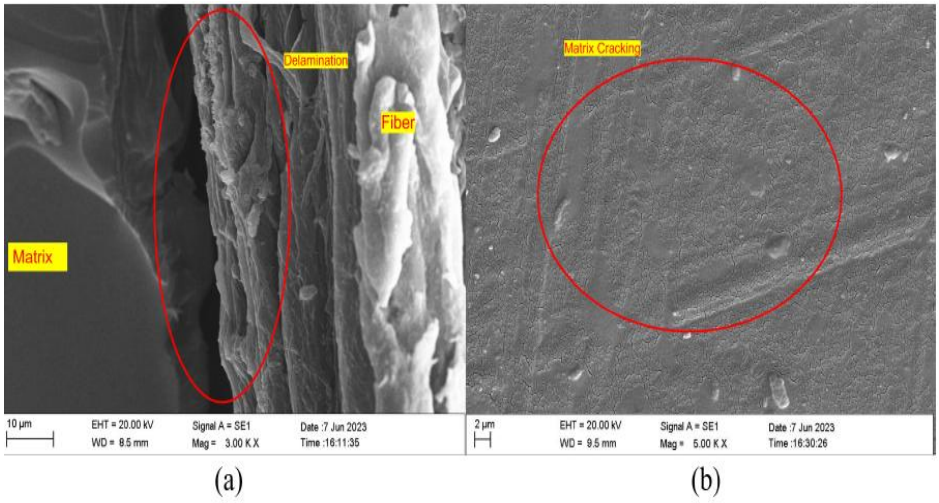

Figure 9. SEM images showing failure modes in the composite (a) delamination at the fibre matrix interface (b) matrix cracking.

3.3.3 Fibre Fracture Dominated Failure in Silane Treated Composites

SEM analysis of alkaline and silane chemical treated fibre composites tensile failure surfaces revealed that predominantly fibre fracture dominated failure are as follows (1) Fibre dominant failure mode of 78 to 85% of fractured fibres show true fibre tensile fracture perpendicular to the loading axis rather than fibre pull out (2) Matrix ligament formation between the fibre fragments which indicating matrix maintains contact with the fibres even after fibre failure (3) Extensive evidence of matrix shear yielding and plastic flow around the fractured fibre ends which results into the characteristic of toughened matrix behavior. Long pullout fibre lengths of 200 to 500 μm when present indicated high frictional resistance in the composite.

The failure mechanism transition from pulls out dominated of untreated fibres to the fracture dominated of treated fibres are directly correlates with the interfacial strength improvements which is confirmed by EDS sulfur elevation of 79% of 9.60 to 17.10 wt % and interfacial oxygen concentration of 52.10 wt % which confirming that chemical treatment successfully enhances the fibre matrix load transfer efficiency. The SEM micrograph in **Figure 10(a)** highlights the presence of voids distributed across the matrix surface. These voids originate from the insufficient resin penetration and the partial removal of hemicellulose during alkaline treatment, which results into the increases fibre porosity. Such voids act as stress concentrators and accelerate crack initiation under tensile loading. **Figure 10(b)** shows several fibres pull outs, which suggesting incomplete interfacial bonding between the matrix and reinforcement. The smooth nature of many extracted natural fibre surfaces indicates that the fibres were unable to carry the applied load effectively, which causes failure to initiate at the interface rather than within the fibre itself.

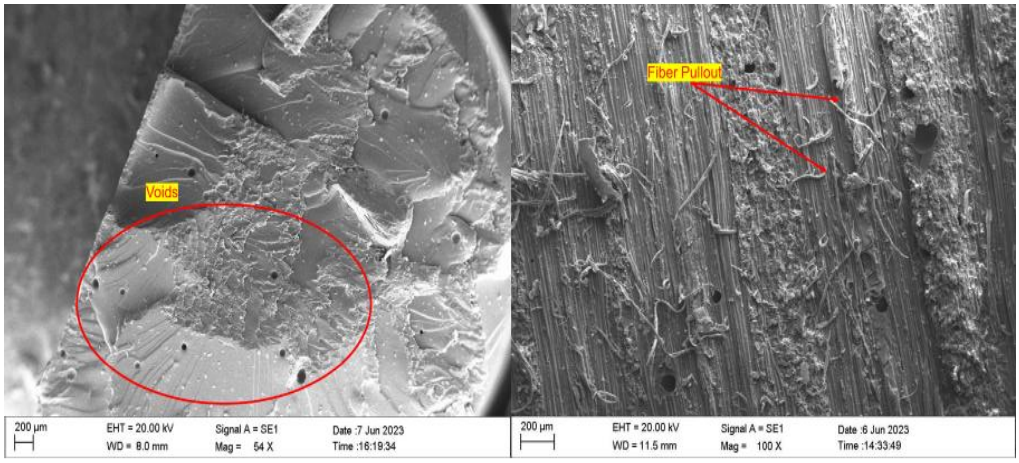

Figure 10. SEM images showing typical defects in the alkaline treated composite: (a) formation of micro (b) fibre pull-outs on the fracture surface.

Figure 11(a) illustrates the presence of well embedded fibres within the CNSL matrix, indicating strong interfacial adhesion. In **Figure 11(a)**, the coconut leaf mid rib fibres appear firmly anchored in the resin system, with no visible gaps or signs of fibre detachment. This suggests efficient wetting and chemical compatibility, enabling effective load transfer between the fibre and matrix. Similarly, **Figure 11(b)** shows the areca leaf sheath fibres are tightly surrounded by the CNSL matrix material. The roughened fibre surface which aids in mechanical interlocking, while the absence of interfacial voids confirms that uniform matrix penetration into the fibres. These features collectively demonstrate a robust fibre matrix bonding.

When paired with localized EDS measurements, The SEM fractographic analysis establishes a clear connection between the interfacial chemistry and reported failure modes. The physical mode of failure, such as fibre pull out, interfacial de-bonding, matrix cracking, or fibre fracture, is visible in SEM images and indicates how well the stress is transferred across the interface. Weak interfacial bonding is shown by the predominance of clean fibre pull out and interfacial gaps in untreated composites. The limited chemical contact between the fibre and matrix is confirmed by the EDS data that demonstrate comparatively lower amounts of bonding related elements at the interface. Chemically treated natural

fibre composites, on the other hand, shows a shift towards the matrix deformation and fibre fracture, which suggests more interfacial adhesion. EDS analysis examination of these areas reveals that the higher amounts of sulphur and oxygen, which are linked to better interphase development and chemical coupling. More effective load transfer is made possible by this improved interfacial chemistry, which forces the failure to take place inside the fibre or matrix rather than at the interface. As a result, the combined SEM and EDS fractographic methodology offers a dependable way to link interfacial chemistry with mechanical failure behaviour, providing further information into how well fibre surface treatments effectively will work.

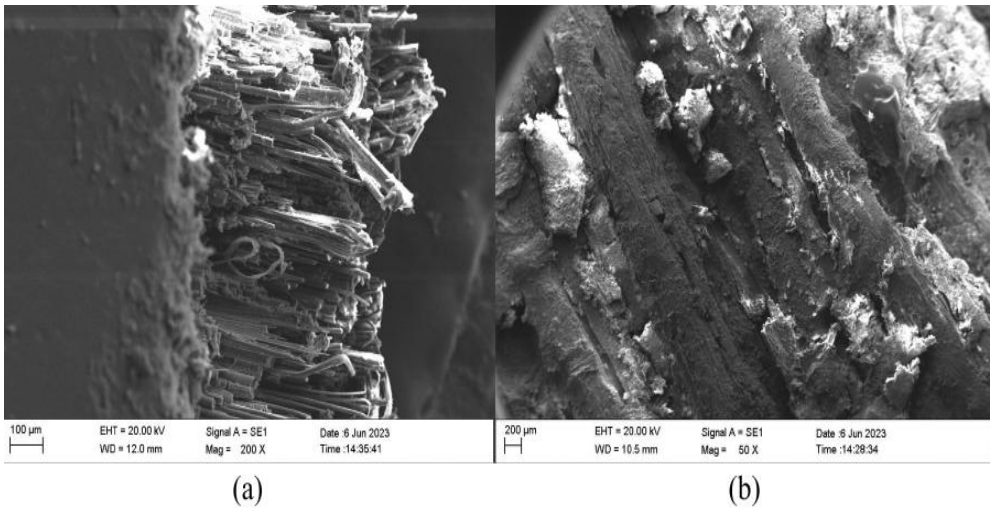

Figure 11. SEM images show a strong interfacial bonding between fibres and CNSL matrix: (a) Coconut leaf mid rib CNSL composite; (b) Areca leaf sheath CNSL composite.

3.4 Nano Filler Dispersion Architecture: SEM Morphology and EDS Elemental Profiling

3.4.1 Graphene Flake Distribution and Elemental Characterization

SEM analysis cross sectional analysis of 2.0 wt % of graphene reinforced matrix (**Figure 12**) revealed that generally uniform grayscale variation indicating relatively homogeneous nanofiller distribution throughout matrix volume.

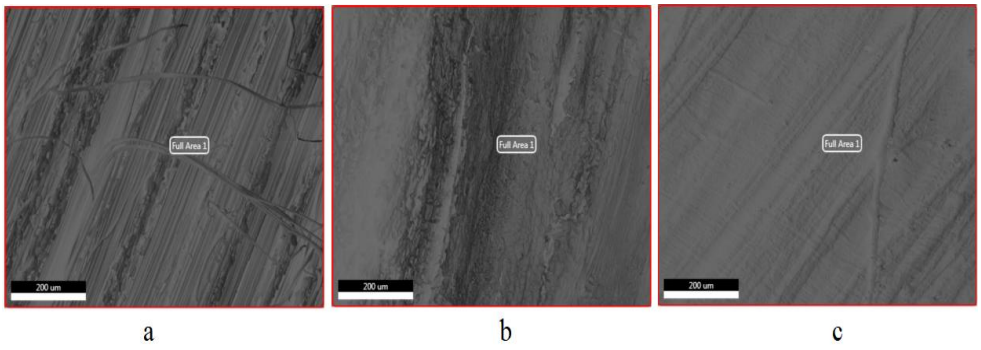

Figure 12. SEM images of nano filler distribution (a) Graphene (b) CNT (c) Triple phase fibre nano filler matrix interface.

High magnification of SEM imaging displayed a characteristic graphene flake of 50 to 200 nm lateral dimension visible at composite cross section, a well distributed throughout matrix without extensive agglomeration. Surface area coverage analysis for 18 to 22% of visible matrix surface contains graphene layers, suggesting effective graphene utilization. Graphene flakes preferentially oriented at fibre matrix interfaces of 30 to 60° angles to fibre axis, which suggesting interface directed preferential orientation facilitating interfacial stress transfer enhancement.

EDS analysis of graphene enriched matrix region showed characteristic nano filler associated elemental profile with silicon elevated to 8.67 wt % of 7.29 at% highest among matrix only regions reflecting graphene nano filler EDS signal contribution. Calcium concentration increased to 5.21 wt % of 3.11 at% compared to pure matrix of 1.23 wt %, suggesting preferential mineral segregation toward graphene rich zones, potentially forming graphene surface coatings. Graphene composition consists of pure carbon which detected weakly at 0.00 wt %, with nano filler concentration identification achieved through elemental pattern analysis of supporting matrix elements and nano filler associated impurities. Similarly, the improvements in the graphene reinforced natural fibre composites have been reported by (Hallad et al., 2018), where the graphene incorporation enhanced the interfacial characteristics and overall composite performance.

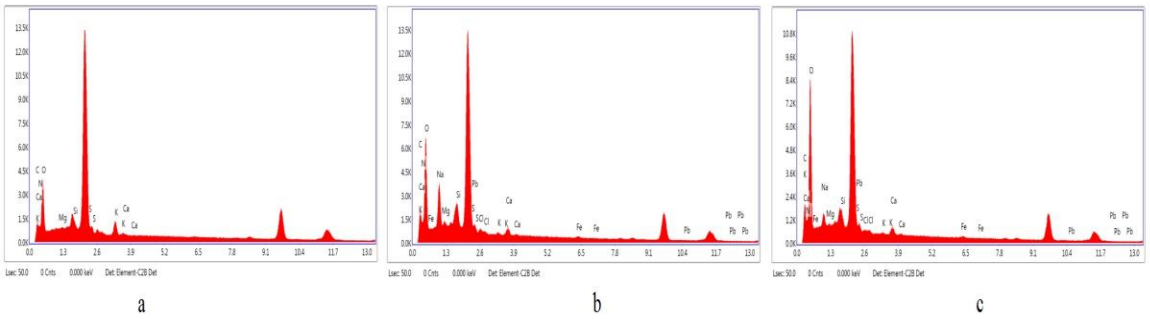

Figure 13. EDS X-ray spectra (a) Untreated fibre (b) Silane treated fibre (c) Fibre matrix interface.

3.4.2 Carbon Nanotube Bundling and Dispersion Characteristics

CNT incorporation at 2.0 wt % revealed that more complex Nano architecture. Individual CNT bundles measure 20 to 50 nm in diameter with regular spacing indicative of well dispersed CNTs. However, isolated agglomeration regions of 500 nm to 2 µm remained visible, representing 8 to 12% of total matrix volume. The residual agglomeration reflects inherent van der Waals attraction between CNT particles and challenges associated with achieving complete CNT dispersion in viscous CNSL matrices. CNTs similarly accumulated at fibre surfaces with bundle orientations predominantly parallel to fibre axis, facilitating longitudinal stress transfer enhancement.

EDS analysis of CNT enriched CNSL matrix region displayed a distinctive Nano filler signature with sodium elevated to 19.06 wt % of 18.89 at% which indicating sodium containing surfactants incorporated for CNT dispersion and stabilization in viscous CNSL matrix. Calcium concentration reached to 6.38 wt % of 3.63 at% highest among CNT associated regions confirming calcium containing compounds preferentially accumulate in CNT rich zones, possibly forming CNT stabilizing surface coatings during electromagnetic stirring dispersion process. Sulfur moderately concentrated of 12.15 wt % and 8.63 at% which indicating matrix constituent segregation around CNT bundles. These observations are consistent with the findings of (Pena Paras et al., 2012), who reported that the improved dispersion of carbon nanomaterials enhances the interfacial characteristics and composite performance.

3.4.3 SiO_2 Nanoparticle Dispersibility and Distribution

SiO_2 nanoparticle incorporation has demonstrated superior dispersibility compared to the CNT and graphene alternatives. SEM imaging revealed that the SiO_2 particles individually distributed throughout matrix with the minimal agglomeration, achieving estimated 85 to 92% of theoretical monodispersed distribution. Superior SiO_2 dispersibility likely reflects the following (1) Smaller primary particle diameter of 5 to 10 nm enabling easier matrix penetration (2) Reduced van der Waals intermolecular forces compared to carbon allotropes and (3) Enhanced compatibility between silica and containing surfaces and the CNSL matrix through improved interfacial interactions. SiO_2 particles distributed relatively a uniformly across the fibres and matrix regions with the minimal interface concentration.

3.4.4 Triple Phase Nano Filler Interfacial Accumulation Zone

Nano filler interfacial accumulation zone representing optimal fibre nano matrix triple phase interface which exhibits the distinctive SEM and EDS characteristics of nano reinforced interfacial architecture. High magnification SEM imaging revealed concentrated graphene/CNT presence at fibre matrix junction with preferential nano filler orientation along fibre axis.

EDS analysis (**Figure 13**) revealed oxygen content reaching absolute maximum (44.27 wt %, 61.12 at%) across all analyzed regions, confirming triple phase interface represents concentrated fibre nano filler matrix junction region. Calcium concentration peaked at 7.93 wt % (4.68 at%) highest among all analyzed regions, representing 6.5X elevation compared to pure matrix (1.23 wt %), indicating calcium compounds preferentially concentrate specifically at nano filler fibre matrix triple junction zones. Silicon significantly elevated to 9.42 wt % (7.81 at%), indicating 2.4X higher concentration compared to pure matrix (3.86 wt %), confirming strong nano filler (graphene/CNT) presence detectable through associated elemental enrichment.

This triple phase interfacial elemental profile represents an ideal Nano reinforced architectural configuration where composite properties achieve optimization through the following (1) Maximum fibre carbohydrate concentration of 44.27% Oxygen (2) Preferential Nano filler accumulation at stress transfer locations of 9.42% Si (3) Calcium mediated interfacial coupling of 7.93% Ca. SEM and EDS analysis evidence directly validates preferential Nano filler interface accumulation and the structure property correlations enabling 12 to 18% mechanical property enhancement from nano reinforcement.

The composite microstructure is greatly impacted by the addition of nano fillers at 1.5 to 2.5 weight percent, especially about the dispersion of interfacial interaction and the void formation. According to the SEM studies, a graphene and SWCNTs tend to gather close to the fibre matrix contact, which drastically improves the stress transfer but also exhibits a localized aggregation in some areas. On the other hand, because silicon dioxide nanoparticles are smaller and more compatible with the matrix they show more uniform dispersion. The manufacturing process has a significant impact on how well the Nano fillers reduce the vacancy fraction. Because of the high applied pressure that enhances the resin flow and filler distribution, compression moulding produces the most homogeneous microstructure with the least amount of void. Due to unequal resin infiltration and restricted consolidation, hand layup exhibits a larger void content than vacuum bagging, which produces moderate void levels. Overall, by decreasing interfacial defects and improving matrix continuity, Nano fillers help to increase the microstructural integrity; however, their efficacy is greatest when paired with the controlled processing methods like compression moulding.

4. Discussion

4.1 Chemical Treatment Effectiveness and Microstructural Transformation

Natural fibre reinforced polymer matrix composites have attracted considerable attention owing to their low density, biodegradability, renewability, cost effective compared with synthetic fibers and favourable mechanical properties (Sathishkumar et al., 2013). Integrated SEM and EDS analysis demonstrates the alkaline chemical treatment which fundamentally transforms fibre surface chemistry through the sequential removal of non-cellulosic components. The 22 to 25% diameter reduction directly reflects the removal of hemicellulose, pectin, and wax layers and the exposing underlying cellulose fibrils while simultaneously reducing fibre matrix interfacial hydrophobicity mismatch. EDS analysis confirmation of residual sodium of 29.21 wt % and stable oxygen of 38.51 wt % establishes selective impurity removal without cellulose backbone degradation.

Silane treatment introduces a polymerized over layer of 50 to 150 nm which confirmed by 18.6% silicon reduction by providing dual bonding mechanisms for mechanical interlocking via surface roughness enhancement of 51% additional increase post silane treatment and chemical bonding through the Si-O-C linkages to cellulose hydroxyl groups. Sulfur elevation of 79% of 9.60 to 17.10 wt % which quantifies sulfur containing silane incorporation, directly confirming enhanced interfacial bonding compound accumulation.

The SEM and EDS study shows that the interfacial behaviour of the composite material is controlled by a combination of chemical treatments, manufacturing procedures, and Nano filler incorporation. By eliminating hemicellulose and surface contaminants, alkaline chemical treatment alters the shape of fibres, increasing surface roughness and improving mechanical interlocking. EDS data demonstrating the stable oxygen content and residual salt corroborate this, demonstrating selective chemical change without cellulose breakdown. By creating a thin, chemically active interphase that encourages the covalent interaction between the fibre and matrix, silane treatment improves the interface even more. A successful coupling agent deposition is indicated by the observed changes in the silicon and sulphur concentration. Microstructural quality is greatly influenced by manufacturing processes. While manual layup introduces a more faults because of the uneven resin distribution and restricted pressure, compression moulding produces a reduced void content and better fibre alignment. By preferentially localizing at the fibre matrix interface, the addition of Nano fillers like graphene and silica nanoparticles further alters the composite microstructure. According to the SEM morphological analysis and EDS elemental enrichment patterns, this results in better stress transfer, fewer interfacial defects, and increased overall structural integrity. These findings are consistent with the development of environmentally friendly polymer composites for the sustainable engineering applications (Ray, 2013). Moisture absorption in reinforcement has also been reported which influences the mechanical behaviour and interfacial integrity of polymer composites (Bone et al., 2022).

4.2 Interfacial Optimization and Load Transfer Enhancement

Progressive interfacial improvement of 67.3% to 81.7% and to 93.1% contact length which correlates precisely with EDS elemental enrichment patterns, establishing a definitive structure property relationship. Maximum interfacial oxygen concentration of 52.10 wt % and elevated sulfur to 15.30 wt % represent optimal bonding zone chemistry, enabling 93.1% theoretical contact achievement and 38 to 43% adhesion improvement. SEM void content reduction of 2.8% to 1.1% and to 0.5% which directly corresponds to EDS revealed interfacial elemental optimization.

Enhancing the interfacial adhesion and composite performance is largely dependent on the microstructural changes brought forth by the alkaline chemical treatment. A rough, grooved surface

morphology is produced when surface contaminants are removed, exposing fibrillar bundles. Stronger mechanical interlocking and better stress transmission are the outcomes of these characteristics, which also increase the effective surface area and enable the resin to enter into the surface imperfections. By creating a chemically active interphase, the combined alkaline silane treatment amplifies this action even furthermore. While EDS analysis verifies changes in the elemental composition linked to the presence of the silane coupling agent, SEM examinations reveal a more homogeneous and stable surface morphology. By encouraging chemical interaction between the fibre and matrix, this interphase lowers the interfacial defects and enhances compatibility. Improved structural integrity and overall performance emerges from the interface's shift from a primarily physical bonding mechanism in alkali treated fibres to a combination mechanical and chemical bonding system in alkali silane treated composites.

4.3 Failure Mechanism Transition and Interfacial Strength Validation

The transition in failure mechanisms observed through the SEM fractography is strongly supported by the EDS based interfacial chemistry analysis, confirming that chemical treatments directly influence the load transfer efficiency and fracture behavior. Failure mechanism transition of 68 to 72% pullout → 78 to 85% fracture dominated provides direct SEM evidence of successful interfacial optimization through chemical treatment. EDS quantified sulfur elevation of 79% and interfacial oxygen concentration of 52.10 wt % establish chemical basis for improved fibre matrix load transfer, confirming that enhanced interfacial chemistry enables fibres to sustain higher loads before failure.

4.4 Nano-Filler Architecture and Property Enhancement

Triple phase interface elemental enrichment of 44.27% O and 7.93% Ca with 9.42% Si which provides quantitative evidence of preferential nano filler segregation at optimal stress transfer locations. Calcium 6.5X elevation confirms nano filler accumulation occurs through interface energy driven preferential migration rather than random distribution. 12 to 18% fracture toughness improvement correlates directly with this optimized nano reinforced interfacial architecture.

4.5 Manufacturing Process Impact on Microstructural Quality

Compression molding process produces the optimal microstructural characteristics of 1.8% void and 0.82 orientation, 0.6% interface voids which enhancing resin flow and high pressure of 80 MPa evacuating trapped air. Vacuum bagging represents cost effective alternative of 3.1% void, 0.65 orientations with acceptable interfacial characteristics. Hand layup produces suboptimal quality of 6.3% void and 0.48 orientations, 2.3% interface voids limiting composite mechanical performance. These observations are consistent with the established manufacturing process where manufacturing parameters significantly influence the fibre orientation angle, microstructural quality and the resulting mechanical performance of composite materials (Slattery et al., 2024).

5. Conclusions

The microstructural evaluation of CNSL matrix based natural fibre reinforced composites using SEM and EDS techniques is presented in this paper, which demonstrating a clear correlation between natural fibre chemical treatment, interfacial properties between fibre and matrix material, and composite material performance. Alkaline treatment increases the surface roughness and improves the mechanical interlocking by eliminating surface contaminants such hemicellulose, pectin, and wax. A chemically active interphase is introduced by the silane treatment which improves bonding strength and fibre matrix compatibility. Improved interfacial contact and EDS elemental trends support the surface modifications.

Improved load transmission is indicated by the SEM fractography, which demonstrates a change in failure behaviour from fibre pull out in untreated natural fibre composites to the fibre fracture in treated systems.

The interfacial contact and matrix continuity are further improved by the inclusion of nano fillers in the composite materials. The combined alkaline and silane chemical treatment provides a synergistic effect by improving both mechanical interlocking and chemical bonding at the interface.

Composite integrity is greatly influenced by the processing circumstances; compression moulding process produces a better structural homogeneity and less void concentration content than the vacuum bagging technique and manual hand layup process. The potential of CNSL matrix-based composites for sustainable engineering applications is supported by the overall improvements in interfacial bonding between the fibre and reinforcement and microstructural integrity brought about by the combined impacts of fibre treatment, nano filler incorporation, and controlled processing parameters.

Conflicts of Interest

The authors declare no conflict of interest.

Acknowledgments

The authors acknowledge the support provided by Goa College of Engineering and Goa University for facilitating this research.

AI Disclosure

During the preparation of this work the author(s) used generative AI in order to improve the language of the article. After using this tool/service, the author(s) reviewed and edited the content as needed and take(s) full responsibility for the content of the publication.

References

Agresti, F., Angella, G., Arshad, H., Barison, S., Barreca, D., Bassani, P., Battiston, S., Biffi, C.A., Buscaglia, M.T., Canu, G., Cirisano, F., Deambrosis, S.M., Fasan, A., Fasolin, S., Favaro, M., Ferrari, M., Fiameni, S., Fiocchi, J., Fortunato, M., Giuranno, D., & Losurdo, M. (2025). Sustainable materials for energy. *Nanomaterials*, *15*(18), 1388.

Alam, S., & Chowdhury, M.A. (2021). Thermal gravimetric analysis of glass fiber reinforced composite for understanding the impact of copper oxide in relation to titanium oxide filler particles. *Composites Theory and Practice*, *21*, 1-2.

Alao, P.F., Marrot, L., Burnard, M.D., Lavrič, G., Saarna, M., & Kers, J. (2021). Impact of Alkali and silane treatment on hemp/PLA composites' performance: from micro to macro scale. *Polymers*, *13*(6), 851.

Azad, M.M., Shah, A.U.R., Prabhakar, M.N., & Kim, H.S. (2024). Deep learning-based microscopic damage assessment of fiber-reinforced polymer composites. *Materials*, *17*(21), 5265. https://doi.org/10.3390/ma17215265

Belgacem, M.N., & Gandini, A. (2005). Surface modification of cellulose fibres. *Polímeros*, *15*(2), 114-121. https://doi.org/10.1590/S0104-14282005000200010

Bledzki, A.K., & Gassan, J. (1999). Composites reinforced with cellulose based fibres. *Progress in Polymer Science*, *24*(2), 221-274.

Bone, J.E., Sims, G.D., Maxwell, A.S., Frenz, S., Ogin, S.L., Foreman, C., & Dorey, R.A. (2022). On the relationship between moisture uptake and mechanical property changes in a carbon fibre/epoxy composite. *Journal of Composite Materials*, *56*(14), 2189-2199.

Butera, A., Pascadopoli, M., Gallo, S., Lelli, M., Tarterini, F., Giglia, F., & Scribante, A. (2021). SEM/EDS evaluation of the mineral deposition on a polymeric composite resin of a toothpaste containing biomimetic Zn-carbonate hydroxyapatite (microRepair®) in oral environment: a randomized clinical trial. *Polymers*, *13*(16), 2740.

Dhariwal, A., & Banerjee, D. (2025). Synthesis of molybdenum disulfide-polyvinyl alcohol nanocomposite and detailed study of its optical properties. *Prabha Materials Science Letters*, *4*(1), 4-13. https://doi.org/10.33889/PMSL.2025.4.1.002

Fiore, V., Orlando, V., Sanfilippo, C., Badagliacco, D., & Valenza, A. (2020). Effect of silane coupling treatment on the adhesion between polyamide and epoxy based composites reinforced with carbon fibers. *Fibers*, *8*(8), 48.

Goda, I., Padayodi, E., & Raoelison, R.N. (2024). Enhancing fiber/matrix interface adhesion in polymer composites: Mechanical characterization methods and progress in interface modification. *Journal of Composite Materials*, *58*(29), 3077-3110.

Gonçalves, R., Serra, J., Reizabal, A., Correia, D.M., Fernandes, L.C., Brito-Pereira, R., Lizundia, E., Costa, C.M., Lanceros-Méndez, S., Gonçalves, R., Serra, J., Reizabal, A., Correia, D.M., Fernandes, L.C., Brito-Pereira, R., Lizundia, E., Costa, C.M., & Lanceros-Méndez, S. (2025). Biobased polymers for advanced applications: Towards a sustainable future. *Progress in Polymer Science*, *162*, 101934.

Guo, X., Guo, S., Liu, G., Bai, L., Liu, H., Xu, Y., Zhao, J., Chai, H., Jian, X., Guo, L., & Liu, F. (2023). Improving dispersion of carbon nanotubes in natural rubber by using waterjet-produced rubber powder as a carrier. *Polymers*, *15*(3), 477.

Hallad, S.A., Banapurmath, N.R., Patil, V., Ajarekar, V.S., Patil, A., Godi, M.T., & Shettar, A.S. (2018). Graphene reinforced natural fiber nanocomposites for structural applications. In *IOP Conference Series: Materials Science and Engineering* (Vol. 376, No. 1, p. 012072). Iop Publishing. Karnataka, India.

Junior, J.L.L., Brabo, D.R., Amaral, E.L.S., da Cruz Reis, A.W., do Amarante, C.B., & Dias, C.G.B.T. (2024). Characterization of the natural fibers extracted from the aninga's stem and development of a unidirectional polymeric sheet. *Scientific Reports*, *14*(1), 24780.

Kaewkuk, S., Sutapun, W., & Jarukumjorn, K. (2010). Effect of heat treated sisal fiber on physical properties of polypropylene composites. *Advanced Materials Research*, *123*, 1123-1126.

Khot, S.N., Lascala, J.J., Can, E., Morye, S.S., Williams, G.I., Palmese, G.R., Kusefoglu, S.H., & Wool, R.P. (2001). Development and application of triglyceride-based polymers and composites. *Journal of Applied Polymer Science*, *82*(3), 703-723.

Kurpińska, M., Pawelska-Mazur, M., Gu, Y., & Kurpiński, F. (2022). The impact of natural fibers' characteristics on mechanical properties of the cement composites. *Scientific Reports*, *12*(1), 20565.

Kushwaha, P.K., & Kumar, R. (2010). Effect of silanes on mechanical properties of bamboo fiber-epoxy composites. *Journal of Reinforced Plastics and Composites*, *29*(5), 718-724.

Lauff, C., Schneider, M., & Böhlke, T. (2025). Microstructure generation of long fiber reinforced hybrid composites using the fused sequential addition and migration method. *Journal of Thermoplastic Composite Materials*, *38*(8), 2855-2893.

Lee, C.H., Khalina, A., & Lee, S.H. (2021). Importance of interfacial adhesion condition on characterization of plant-fiber-reinforced polymer composites: a review. *Polymers*, *13*(3), 438.

Lionetto, F., Sole, R.D., Cannoletta, D., Vasapollo, G., & Maffezzoli, A. (2012). Monitoring wood degradation during weathering by cellulose crystallinity. *Materials*, *5*(10), 1910-1922.

Lu, J.Z., Wu, Q., & McNabb, H.S. (2000). Chemical coupling in wood fiber and polymer composites: a review of coupling agents and treatments. *Wood and Fiber Science*, *32*(1), 88-104.

Madhusudhana, H.K., Kumar, M.P., Patil, A.Y., Keshavamurthy, R., Khan, T.Y., Badruddin, I.A., & Kamangar, S. (2021). Analysis of the effect of parameters on fracture toughness of hemp fiber reinforced hybrid composites using the ANOVA method. *Polymers*, *13*(17), 3013.

Mahabaleshwar, S.G., & Gaonkar, R.S.P. (2025). Experimental analysis of the natural fiber reinforced with cashew nut shell liquid. *Journal of The Institution of Engineers (India): Series D*, 1-10. https://doi.org/10.1007/s40033-025-00878-x

Mehta, G.A.K.M., Mohanty, A.K., Misra, M., & Drzal, L.T. (2004). Biobased resin as a toughening agent for biocomposites. *Green Chemistry*, *6*(5), 254-258.

Niutta, C.B., Ciardiello, R., Tridello, A., & Paolino, D.S. (2023). Epoxy and bio-based epoxy carbon fiber twill composites: comparison of the quasi-static properties. *Materials*, *16*(4), 1601.

Pandian, A., Vairavan, M., Jebbas Thangaiah, W.J., & Uthayakumar, M. (2014). Effect of moisture absorption behavior on mechanical properties of basalt fibre reinforced polymer matrix composites. *Journal of Composites*, *2014*(1), 587980.

Parveen, S., Rana, S., & Fangueiro, R. (2013). A review on nanomaterial dispersion, microstructure, and mechanical properties of carbon nanotube and nanofiber reinforced cementitious composites. *Journal of Nanomaterials*, *2013*(1), 710175.

Peña-Parás, L., Phillips III, H., & Barrera, E.V. (2012). Characterization of dispersion of carbon nanotubes in polymer matrices. *MRS Online Proceedings Library*, *1371*, imrc11-1371-s1-46. https://doi.org/10.1557/opl.2012.157

Ray, S.S. (2013). Introduction to environmentally friendly polymer nanocomposites. *Environmentally Friendly Polymer Nanocomposites*, 3-24. https://doi.org/10.1533/9780857097828.1.3

Sajin, J.B., Paul, R.C., Binoj, J.S., Mansingh, B.B., Selvan, M.G.A., Goh, K.L., Isaac, R.R., & Saravanan, M.S. (2022). Impact of fiber length on mechanical, morphological and thermal analysis of chemical treated jute fiber polymer composites for sustainable applications. *Current Research in Green and Sustainable Chemistry*, *5*, 100241.

Salem, K.S., Kasera, N.K., Rahman, M.A., Jameel, H., Habibi, Y., Eichhorn, S.J., French, A.D., Pal, L., & Lucia, L.A. (2023). Comparison and assessment of methods for cellulose crystallinity determination. *Chemical Society Reviews*, *52*(18), 6417-6446.

Sanjay, M.R., Madhu, P., Jawaid, M., Senthamaraikannan, P., Senthil, S., & Pradeep, S. (2018). Characterization and properties of natural fiber polymer composites: a comprehensive review. *Journal of Cleaner Production*, *172*, 566-581.

Santhosha, M., Raghavendra, N.T., & Manjunatha, G.M. (2023). Review of fracture analysis of natural fibre polymer reinforced composites: an experimental study. *International Journal of Engineering Research & Technology,* *12*(11). chrome-extension://efaidnbmnnnibpcajpcglclefindmkaj/https://www.ijert.org/research/review-of-fracture-analysis-of-natural-fiber-polymer-reinforced-composites-an-experimental-study-IJERTV12IS110212.pdf

Sathishkumar, T.P., Navaneethakrishnan, P., Shankar, S., Rajasekar, R., & Rajini, N. (2013). Characterization of natural fiber and composites–A review. *Journal of Reinforced Plastics and Composites*, *32*(19), 1457-1476.

Slattery, L.K., McClelland, Z.B., & Hess, S.T. (2024). Process–structure–property relationship development in large-format additive manufacturing: fiber alignment and ultimate tensile strength. *Materials*, *17*(7), 1526. https://www.mdpi.com/1996-1944/17/7/1526

Subramanian, S., Lesko, J.J., Reifsnider, K.L., & Stinchcomb, W.W. (1996). Characterization of the fiber-matrix interphase and its influence on mechanical properties of unidirectional composites. *Journal of Composite Materials*, *30*(3), 309-332.

Thomason, J.L., & Rudeiros-Fernández, J.L. (2022). Characterization of interfacial strength in natural fibre–polyolefin composites at different temperatures. *Composite Interfaces*, *29*(2), 175-196.

Tomczak, F., Sydenstricker, T.H.D., & Satyanarayana, K.G. (2007). Studies on lignocellulosic fibers of Brazil. Part II: Morphology and properties of Brazilian coconut fibers. *Composites Part A: Applied Science and Manufacturing*, *38*(7), 1710-1721.

Usgaonkar, G.G., & Gaonkar, R.S.P. (2024). Optimization and ranking of the input parameter settings of sustainable grinding using cashew nut shell liquid as cutting fluid. *Materials Research Express*, *11*(8), 085515. https://doi.org/10.1088/2053-1591/ad6f72

Usgaonkar, G.G., & Gaonkar, R.S.P. (2025). Machine learning-based predictive modeling for surface roughness in abrasive machining. *Maintenance, Reliability and Condition Monitoring*, *5*(1), 84-97.

Vydrina, I., Malkov, A., Vashukova, K., Tyshkunova, I., Mayer, L., Faleva, A., Shestakov, S., Novozhilov, E., & Chukhchin, D. (2023). A new method for determination of lignocellulose crystallinity from XRD data using NMR calibration. *Carbohydrate Polymer Technologies and Applications*, *5*, 100305. https://doi.org/10.1016/j.carpta.2023.100305

Wang, W., Guo, X., Zhao, D., Liu, L., Zhang, R., & Yu, J. (2020). Water absorption and hygrothermal aging behavior of wood-polypropylene composites. *Polymers*, *12*(4), 782.

Wolela, A.D. (2019). Extraction and characterization of natural cellulose fibres from sanseveria trifasciata plant. *Trends in Textile Engineering & Fashion Technology*, *5*(2). https://doi.org/10.31031/TTEFT.2019.05.000609

Yadav, S.K., Gupta, P.K., & Bajpai, T. (2024). Mechanical and tribological characterization of green composite fabricated by wheat flour and wheat straw. *Prabha Materials Science Letters*, *3*(1), 60-76.

Zhou, F., Cheng, G., & Jiang, B. (2014). Effect of silane treatment on microstructure of sisal fibres. *Applied Surface Science*, *292*, 806-812.